JBC RESEARCH ARTICLE

Chaperone-mediated disaggregation of infectious prions releases particles that seed new prion formation in a strain-specific manner

Received for publication, July 25, 2024, and in revised form, November 6, 2024 Published, Papers in Press, December 9, 2024,
https://doi.org/10.1016/j.jbc.2024.108062

Daniel Shoup* and **Suzette A. Priola**

From the Rocky Mountain Laboratories, Laboratory of Neurological Infections and Immunity, National Institute of Allergy & Infectious Diseases, National Institutes of Health, Hamilton, Montana, USA

Reviewed by members of the JBC Editorial Board. Edited by Ursula Jakob

The mammalian prion protein can form infectious, nonnative, and protease resistant aggregates (PrP^D), which cause lethal prion diseases like human Creutzfeldt-Jakob disease. PrP^D seeds the formation of new infectious prions by interacting with and triggering the refolding of the normally soluble mammalian prion protein, PrP^C, into more PrP^D. Refolding of misfolded proteins in the cell is carried out by molecular chaperones such as Grp78. We have recently shown that Grp78 sensitizes PrP^D to proteases, indicating structural alterations and leading to its degradation. However, the process of chaperone-mediated PrP^D disaggregation, the chaperones involved, and the effect of disaggregation on PrP^D seeding activity are unclear. We have now monitored the structural modification, disaggregation, and seeding activity of PrP^D from two mouse adapted prion strains, 22L and 87V, in the presence of Grp78 and two forms of the Hsp110 disaggregase chaperone family, Hsp105 and Apg-2. We found that both forms of Hsp110 induced similar amounts of disaggregation and structural change in the protease resistant cores of PrP^D from both strains. However, 22L PrP^D was more susceptible to destabilization and disaggregation by the chaperones than 87V. Surprisingly, despite disaggregation of both strains, only the 22L PrP^D aggregates released by the chaperones had seeding activity, with both forms of Hsp110 enhancing the Grp78 mediated release of these aggregates. Our data show that disassembly of PrP^D by Grp78 and Hsp110 chaperones can release seeding particles of PrP^D in a strain-specific manner, potentially facilitating prion replication and spread.

Transmissible neurodegenerative prion diseases such as chronic wasting disease in deer, scrapie in sheep, and Creutzfeldt-Jakob disease in humans are caused by prions (1). A key step in prion disease pathogenesis is the continuous accumulation of a mammalian prion protein with a nonnatively folded and infectious conformation (PrP^D) that is the primary, if not sole, component of the infectious prion (2). During prion disease, the protease sensitive natively folded prion protein (PrP^C) interacts with aggregated PrP^D, resulting in PrP^C both incorporating into and acquiring the nonnative conformation of the PrP^D aggregate (2, 3). Different nonnative and infectious conformations of PrP^D are referred to as strains as they can vary in their structure and biochemical properties (3–6) as well as in the pathologies they induce during infection (7, 8). Despite these differences, most strains of PrP^D form large and insoluble aggregates that are structurally very stable and resistant to proteolytic degradation (2).

PrP^D persists and accumulates in cellular environments (9–12) despite the presence of molecular chaperones capable of unfolding and disassembling nonnative, *i.e.* misfolded, protein aggregates (13–15) as well as proteolytic machinery capable of degrading protein that cannot be repaired by chaperones (16–18). In mammals, chaperone-mediated disaggregation is performed by members of the Hsp70 chaperone family and their cochaperones (13, 19, 20). These are ATP driven protein clamps (21–24) that forcibly unfold protein clientele (15, 25–27) with the help of their protein recruitment cochaperones and nucleotide exchange factors (15, 24, 25, 28, 29). Hsp70s and their cochaperones are universal components of cellular proteostasis systems that constantly protect cells from a wide range of nonnative and aggregated proteins. While the high structural and conformational stability of PrP^D might be expected to make it recalcitrant to chaperone activity, the Hsp70 system has been found to play a role in prion biology (28, 30). Increasing the cellular concentration of Hsp70s, like Grp78, has been shown to reduce the concentration of PrP^D in chronically infected cells (30). This observation supports the possibility that PrP^D persists in part because of insufficient chaperone expression or activity. However, cells are not cured of infectious prions by increasing the concentration of chaperones (30), indicating that the relationship between chaperones and prions is more complex.

Propagation of PrP^D is dependent upon both continuous conversion of PrP^C and processes that increase the number of aggregates with seeding activity by fragmenting larger PrP^D aggregates into smaller ones (31, 32). While molecular chaperones have been found to fragment and thus promote the propagation of disease related tau (33), α-synuclein (34), and sup35 aggregates (35), the mechanism by which PrP^D is fragmented and the role of chaperones in prion propagation is poorly understood. PrP^D can be found at the cell surface (10, 12)

* For correspondence: Daniel Shoup, daniel.shoup@nih.gov.

as well as within the endosomal trafficking network and it is known to accumulate in lysosomes (11, 12). Both conversion of PrP^D and its subsequent disaggregation, potentially *via* the activity of noncytoplasmic chaperones, could therefore occur in any of these cellular compartments. In addition, PrP^D disassembled during endosomal trafficking is mostly protease resistant (36, 37), suggesting that the process of disaggregation after endocytosis could generate additional particles with seeding activity that could in turn promote the propagation of PrP^D. In a more recent study of how the cell surface chaperones Grp78, Hsp90, and their cochaperones modified PrP^D from two mouse adapted prion strains, 22L and 87V, we used susceptibility to proteases as an indicator of structural change. We found that chaperones significantly reduced the protease resistance of PrP^D from both strains, indicating structural modifications, but still failed to disaggregate the majority of 22L and 87V PrP^D (28). Disaggregation of 22L PrP^D by Grp78, Hsp90, and cochaperones was improved when pretreated with proteinase K (PK), suggesting that disaggregation of PrP^D in cellular environments may result from cycles of exposure to chaperones and proteases (28). However, Grp78 and Hsp90 are not the only chaperones present extracellularly and cointeraction between these chaperones and other extracellular chaperones could facilitate more efficient disaggregation of PrP^D.

Numerous mammalian proteins, such as TRIM (38) and DAXX (39), possess a putative disaggregase activity under specific conditions. However, many of these putative disaggregases still cooperate with the Hsp70 chaperone network (40) and, when tested independently, possess comparatively lower chaperone activity when compared to Hsp70 systems (38, 39). Additionally, nonheat shock protein disaggregases are typically cytoplasmic (41, 42) and are not known to localize where prions propagate along the cell surface and endosome. Disassembly of nonnative protein aggregates in higher metazoans typically also requires the activity of the cytoplasmic chaperone Hsp110, which is a nucleotide exchange factor for Hsp70 chaperones that also possesses an Hsp70 substrate binding domain (13, 20, 29). Two members of the Hsp110 chaperone family that predominately drive disaggregation in mammals are Apg-2 and Hsp105, though the expression of these chaperones can vary with cell type (43–45). Secretion of Hsp110 chaperones has been observed in specific cancer cells (46), intestinal cells (47), and cells that are stressed (48, 49) but they are not consistently found extracellularly. Despite the different localization of Hsp110 chaperones and PrP^D, overexpression of Hsp110 in *Drosophila* was found to reduce the amount of both aggregated PrP^D and aggregates with seeding activity (50). While the effect of Hsp110 overexpression on PrP^D may have directly led to the reduction in PrP^D concentrations through disaggregation, the effect could also have been indirect as Hsp110 regulates expression and secretion of several proteins as well as regulating clathrin-mediated endocytosis (47, 51). Thus, a detailed analysis of the disaggregation activity of Hsp110 chaperones *in vitro* would help to directly determine whether Hsp70/Hsp110 can mediate disaggregation of PrP^D and its seeding activity.

In this work, we investigated whether the Hsp70 variant Grp78, the cochaperone DnaJC1, and two members of the Hsp110 chaperone family, Agp-2 and Hsp105, were able to disassemble larger 22L and 87V PrP^D aggregates into smaller PrP^D aggregates with seeding activity. Sucrose sedimentation was used to evaluate the amount and relative size of PrP^D solubilized by chaperones, and the real-time quaking-induced conversion (RT-QuIC) assay was used to assess seeding activity in solubilized PrP^D. We found that while 10 to 35% of 22L and 87V PrP^D was disassembled by Grp78 in the presence of either Apg-2 or Hsp105, chaperones liberated particles with seeding activity only from 22L PrP^D. Our data indicate that while chaperones are capable of disassembling PrP^D, their ability to disrupt the seeding properties of PrP^D may be limited in a strain-specific manner.

Results

Hsp105 and Apg-2 promote both the loss of protease resistance and disaggregation of PrP^D by Grp78 in a strain-specific manner

We first asked if Hsp105 and Apg-2 facilitated the Grp78 mediated structural modification of PrP^D from different prion strains. To monitor PrP^D structural changes, we assessed the susceptibility of PrP^D to protease digestion, a well-established method for monitoring protein structural modification and destabilization (52–54) that is commonly used in the prion field (52–56). We used immunoblot analysis to quantify changes in protease resistance of sodium phosphotungstic acid hydrate (PTA) precipitated 22L and 87V PrP^D following exposure to Grp78 and DnaJC1 with and without either Hsp105 or Apg-2 (Fig. 1). Since our previous work had shown that proteolytic digestion of 22L and 87V PrP^D could influence chaperone-mediated modification of both strains (28), we compared the influence of chaperones on PrP^D that was or was not pretreated with PK, respectively referred to as the "protease resistant core" and "total PrP^D".

Both total PrP^D and the PrP^D protease resistant core were incubated with or without chaperones for 30 min before being treated with PK. Three independent PK treated (Fig. 1) samples were then analyzed *via* Western blot developed with the 6D11 anti-PrP antibody (Fig. 1, left panels). For both strains, the PK resistance of the PrP^D n terminus up to residue 109 was not significantly reduced in the presence of Grp78 and DnaJC1 regardless of PK pretreatment (Fig. 1, *A* and *B*). Both Hsp105 and Apg-2 reduced the PK resistance of total PrP^D from both strains, with 22L (Fig. 1*A*, right panel) showing a greater sensitivity to chaperone activity than 87V (Fig. 1*B*, right panel). These differences were not due to variability in the amount of PrP^D in the starting samples as each sample contained similar levels of PrP^D (Fig. S1). However, while the protease resistant core of 22L PrP^D up to residues 93 to 109 was mostly resistant to destabilization by Hsp105 but not Apg-2 (Fig. 1*A*, right panel), the same region of 87V was resistant to destabilization by both Hsp105 and Apg-2 (Fig. 1*B*, right panel). These data are consistent with previous work showing that 87V is more

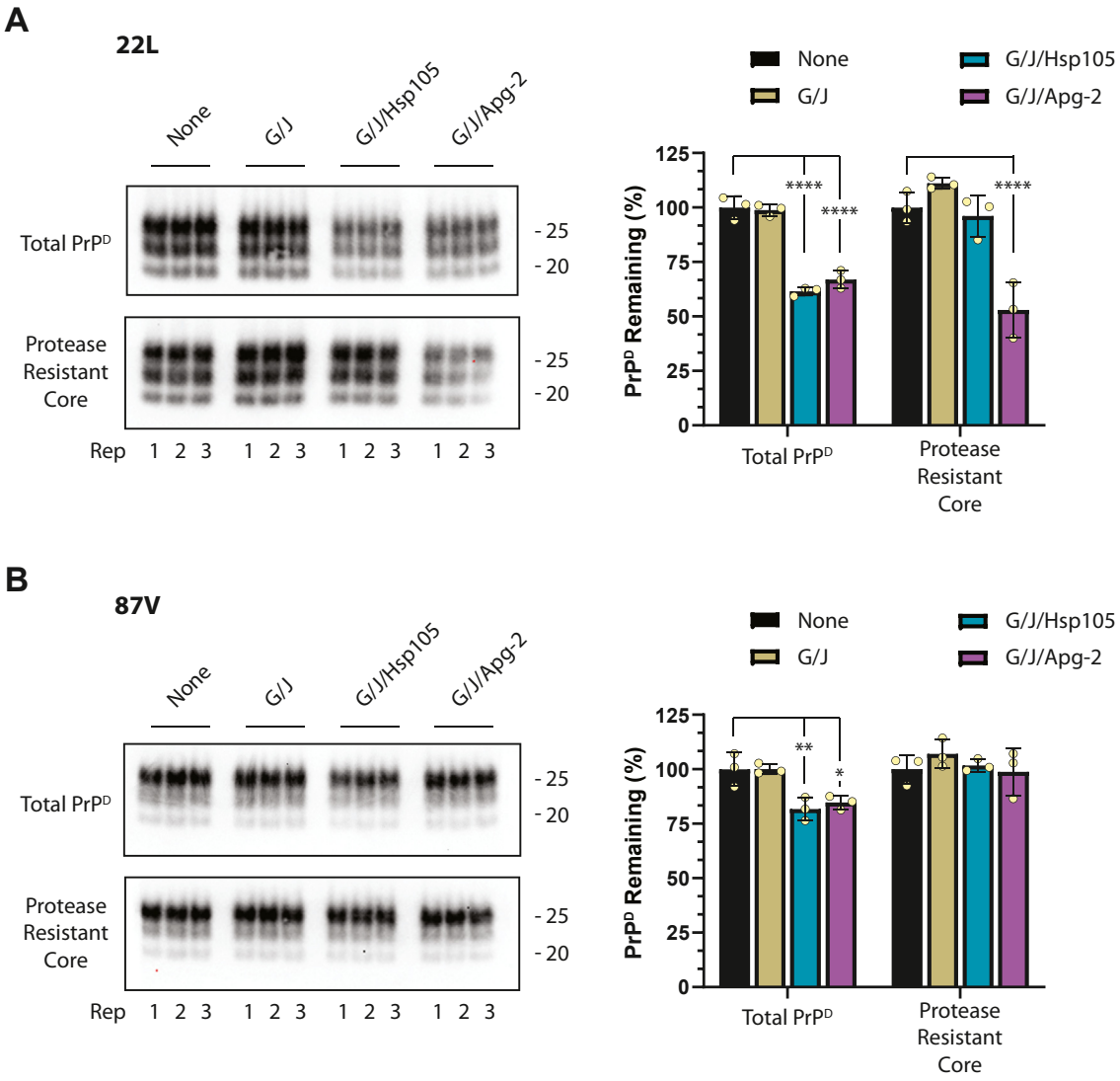

Figure 1. Hsp105 and Apg-2 promote the loss of PrP^D PK resistance in a strain-specific manner. 22L and 87V PrP^D precipitated with PTA from prion infected mouse brain homogenates was incubated without chaperones (none) or in the presence of Grp78 and DnaJC1 (G/J) with either Hsp105 (G/J/Hsp105) or Apg-2 (G/J/Apg-2) for 30 min. Samples were then PK treated for 1 h before being analyzed by Western blot. Immunoblots (*left* panels) show the influence of chaperones on total PrP^D (*upper* blots) and its protease resistant core (*lower* blots) from both (*A*) 22L and (*B*) 87V. All samples contained ATP and an ATP regeneration system. All blots were probed with the anti-PrP antibody 6D11 (epitope 93–109) and molecular mass markers for 25 kDa (*upper* marker) and 20 kDa (*lower* marker) are shown to the right of each blot. The bar plots (*right* panels) show the average percentage of protease resistant PrP^D remaining after exposure to no chaperones (none, *black bars*), G/J (*gold bars*), G/J/Hsp105 (*blue* bars), or G/J/Apg-2 (*purple bars*), followed by PK treatment. Percentages were calculated by normalization to samples not exposed to chaperones (none) run on the same gels. For all graphs, data were calculated from n = 3 from each of the three replicates (Rep) shown for each condition and are given as mean ± standard deviation. Individual data points are shown in *yellow*. Significance was determined using a one-way ANOVA with Tukey's multiple comparisons. $p^* = 0.02$, $p^{**} = 0.007$, and $p^{****} = < 0.0009$. PK, proteinase K; PTA, phosphotungstic acid.

structurally stable (37) and recalcitrant to chaperone activity (28), while the greater effectiveness of Apg-2 on the protease resistant core of 22L PrP^D compared to Hsp105 indicates that the ability to destabilize PrP^D can vary between members of the Hsp110 chaperone family.

Previous work has shown that loss of protease resistance does not necessarily correlate with disaggregation (28). Using an immunoblot based sedimentation assay, we therefore tested whether the addition of either Hsp105 or Apg-2 facilitated disaggregation of 22L and 87V PrP^D in the presence of both Grp78 and DnaJC1. Samples of total PrP^D and its protease resistant core containing similar levels of PrP^D (Fig. S2) were incubated with the chaperones for 30 min before samples were centrifuged to separate large PrP^D aggregates from those liberated by chaperone activity. In order to quantify the amount of 22L and 87V disaggregated by chaperones, samples of PrP^D that were neither centrifuged nor exposed to chaperones were analyzed on the same Western blot alongside supernatant samples (Fig. 2) of PrP^D exposed to both Grp78 and DnaJC1 with and without either Hsp105 or Apg-2. Similar to previous studies with Grp78 and cochaperones (28), the vast majority of 22L and 87V PrP^D was not disaggregated in the presence of only Grp78 and DnaJC1 (Fig. 2, *A* and *B*, lanes labeled G/J). However, a significant amount of disaggregation

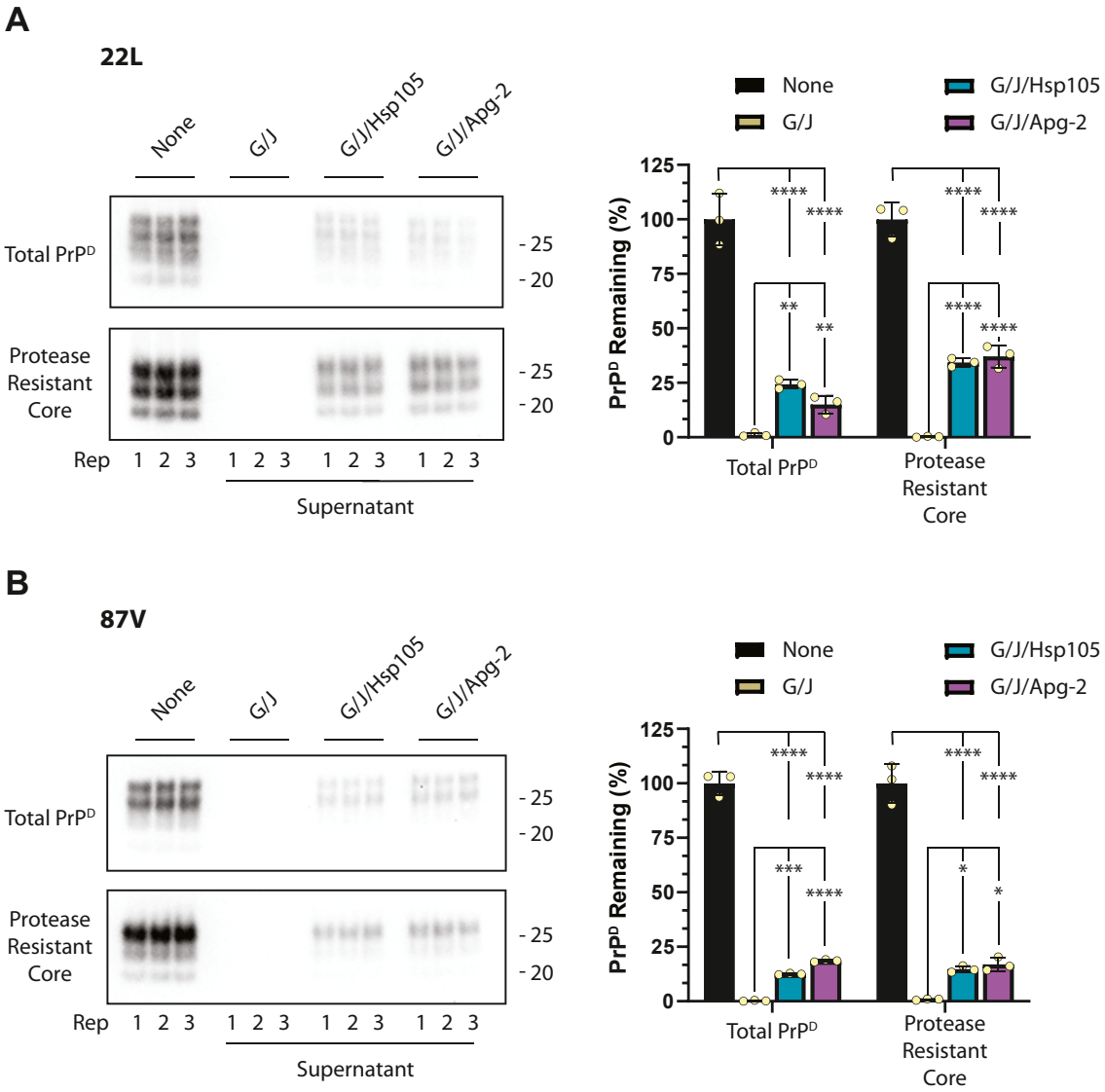

Figure 2. Disaggregation of 22L and 87V PrP^D can be mediated by Grp78 and DnaJC1 in the presence of either Hsp105 or Apg-2. Total PrP^D (*upper* blots) and its protease resistant core (*lower* blots) from (*A*) 22L and (*B*) 87V were PTA precipitated and incubated with Grp78 and DnaJC1 (G/J) and either Hsp105 (G/J/Hsp105) or Apg-2 (G/J/Apg-2) for 30 min. Control samples without either chaperones or centrifugation (none) were also incubated for 30 min. All samples contained ATP and an ATP regeneration system. Chaperone samples were centrifuged over 10% sucrose to pellet insoluble aggregates. Chaperone solubilized monomer and small aggregates remained in the supernatant, which was analyzed by Western blot (*left* panels) alongside control samples that were not centrifuged or exposed to chaperones to determine the amount of prion protein liberated by chaperone activity. All blots were probed with the anti-PrP antibody 6D11 and molecular mass markers for 25 kDa (*upper* marker) and 20 kDa (*lower* marker) are shown to the right of each blot. The bar plots (*right* panels) show the average percentage of PrP^D present in the supernatant after exposure to no chaperones (none, *black* bars), G/J (*gold* bars), G/J/Hsp105 (*blue* bars), or G/J/Apg-2 (*purple* bars). Percentages were calculated by normalization to samples not exposed to chaperones or centrifuged. For all graphs, data were calculated from n = 3 replicate (Rep) samples for each condition shown and are given as mean ± standard deviation. Individual points are shown in *yellow*. Significance was determined using a one-way ANOVA with Tukey's multiple comparisons. p^* = 0.01 to 0.04, p^{**} = 0.005 to 0.009, p^{***} = 0.003, and p^{****} = < 0.0009. PTA, phosphotungstic acid.

of PrP^D ranging from 20 to 35% for 22L (Fig. 2*A*, right panel) and 10 to 20% for 87V (Fig. 2*B*, right panel) was observed when either Hsp105 or Apg-2 were present. There was little difference in the amount of PrP^D solubilized in the presence of Hsp105 and Apg-2 in each sample set (Fig. 2, right panels). However, similar to our earlier studies (28), the protease resistant core of 22L PrP^D was more susceptible to disaggregation than total PrP^D samples (Fig. 2). Overall, the data demonstrate that Grp78 and two members of the Hsp110 chaperone family can facilitate disaggregation of prions from at least two different scrapie strains.

Disaggregation of 22L PrP^D facilitated by Hsp105 and Apg-2 releases particles capable of seeding new PrP^D

Prion replication and spread is likely dependent upon the generation of small oligomers/aggregates of PrP^D from larger PrP^D aggregates that can then seed the formation of new PrP^D (31, 32). How these seeding oligomers are generated is poorly understood, but our data suggest that chaperone activity can lead to the release of smaller PrP^D particles (Fig. 2). We therefore considered the possibility that these smaller PrP^D particles could have seeding activity. In order to determine if PrP^D particles with seeding activity were released during

disaggregation with Grp78 and DnaJC1 in the presence of either Hsp105 or Apg-2, we first tested 22L total PrP^D (Fig. 3) for changes in seeding activity using the RT-QuIC assay. The individual traces from replicates of each sample type were averaged and are displayed in the line plots shown in Figure 3, *A–D*. Different samples were then compared by calculating the

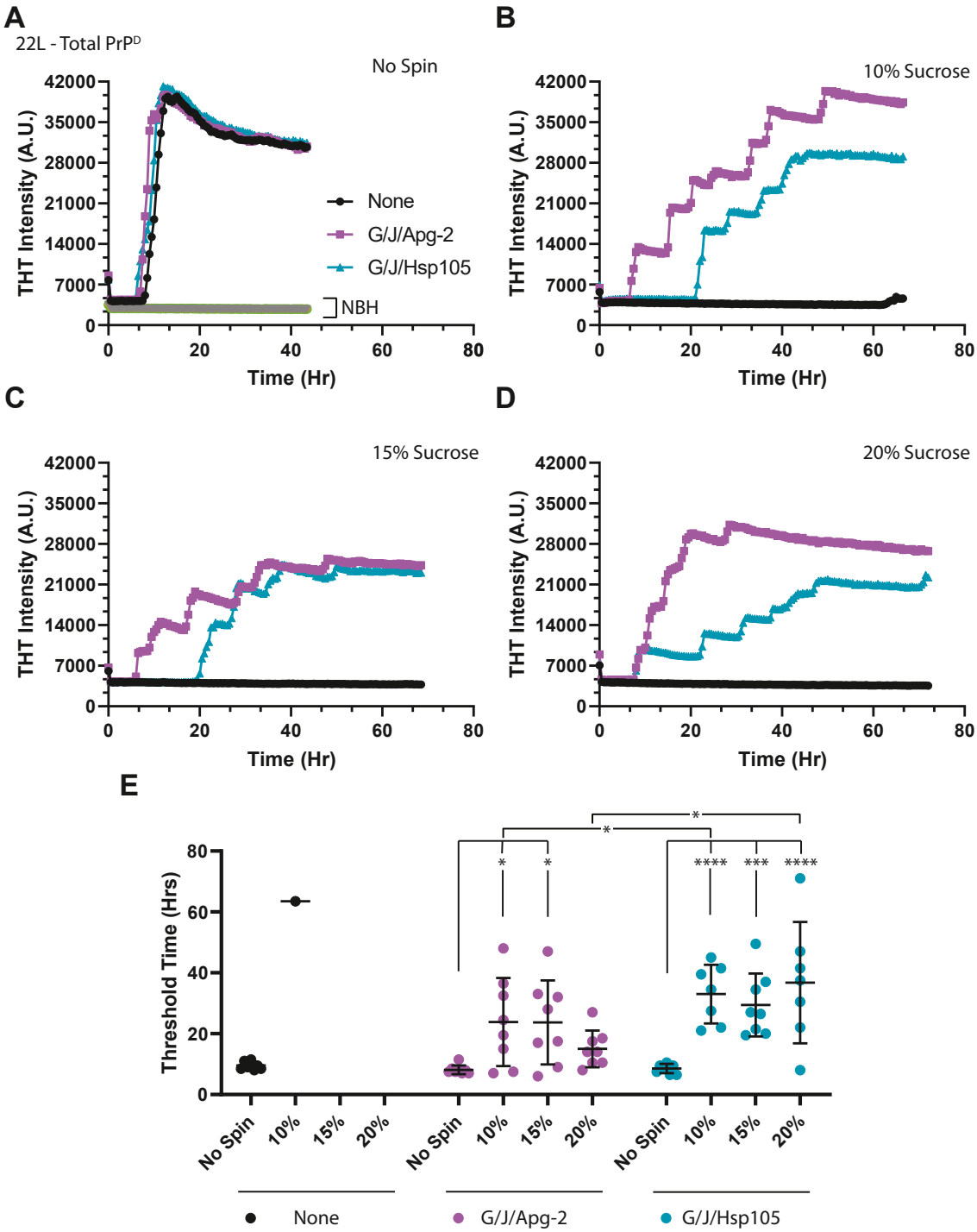

Figure 3. Exposure of total 22L PrP^D to chaperones yields PrP^D particles with seeding activity. The presence of seeding particles in untreated samples of 22L total PrP^D (None, *black lines* and *circles*) or samples that were exposed to the chaperones Grp78 and DnaJC1 in the presence of either Hsp105 (G/J/Hsp105, *blue lines* and *triangles*) or Apg-2 (G/J/Apg-2, *purple lines* and *squares*) was analyzed by real-time quaking-induced conversion. *A*, seeding activity in 22L total PrP^D samples prior to centrifugation over sucrose (no spin). Seeding activity in the supernatant of 22L total PrP^D samples centrifuged over layers of (*B*) 10, (*C*) 15, and (*D*) 20% sucrose. The brackets in (*A*) indicate uninfected, normal brain homogenate (NBH) control samples, that were, or were not, exposed to each chaperone set. The plots shown are based on the average of eight independent samples. *E*, threshold times in hours (Hrs) for the data from panels *A–D*. Shown is the time for THT fluorescence in each well to rise above a threshold set to two times the base line fluorescence of each well. For each experimental condition (none; *black circles*, G/J/Apg-2; *purple circles*, G/J/Hsp105; *blue circles*), the number of total positive wells, as well as the average, and standard deviation threshold times, are given in Table 1. All samples were incubated with ATP and an ATP regeneration system. Significance was determined using a two-way ANOVA with Tukey's multiple comparisons. p^* = 0.01 to 0.04, p^{***} = 0.003, and p^{****} = < 0.0009. THT, thioflavin T.

average time each RT-QuIC reaction took to cross a threshold set to two times the baseline of each sample (Fig. 3*E*). We initially tested whole unfractionated samples but found no significant difference in seeding activity (Fig. 3*A*).

We next used centrifugal sedimentation in increasing concentrations of sucrose (Fig. 3, *B–D*) to separate larger aggregates from smaller aggregates in the supernatant. This allowed us to look specifically for seeding activity across a range of smaller PrP^D particle sizes released from the aggregate. The number of positive wells, average threshold times, and standard deviations are shown in Table 1. The data show 22L PrP^D seeding activity in the supernatants of chaperone-treated samples centrifuged through 10 to 20% sucrose, with no significant seeding activity in samples not exposed to chaperones (Table 1, Fig. 3, *B–D*). The lower time to threshold for total PrP^D from 22L that had been treated with Grp78/DnaJC1 and Apg-2 suggested that it contained significantly more seeding activity than samples treated with Grp78/DnaJC1 and Hsp105 (Table 1 and Fig. 3*E*). Thus, treatment of total 22L PrP^D with chaperones led to the release of particles capable of seeding the formation of new PrP^D.

The protease resistant core of 22L PrP^D was more susceptible to disaggregation by chaperones than total PrP^D samples (Fig. 2*A*), suggesting the possibility that a greater number of PrP^D particles with seeding activity were being released from the aggregate. We therefore determined the seeding activity of PrP^D released from the protease resistant core of 22L PrP^D following treatment with Grp78 and DnaJC1 in the presence of either Hsp105 or Apg-2 (Fig. 4). In general, the data were similar to those from 22L total PrP^D incubated with chaperones (Fig. 3). Nonpelleted samples showed no difference in seeding activity (Table 1 and Fig. 4, *A* and *E*), while seeding activity was almost exclusively detected in supernatant samples exposed to chaperones (Table 1, Fig. 4, *B–E*). A few wells from samples not exposed to chaperones showed some activity (Fig. 4, *C–E*, black lines and circles), indicating that protease treatment alone may have altered the size distribution of 22L PrP^D to create some particles with seeding activity, albeit much less effectively than samples incubated with chaperones (Fig. 4*E*). As with total PrP^D from 22L, the seeding particles from the 22L PrP^D protease resistant core were relatively small, with no difference in seeding activity between samples pelleted through 10 to 20% sucrose (Table 1, Fig. 4, *B–E*). In contrast to total PrP^D, there was no significant difference in the amount of seeding activity released from samples of the protease resistant core of 22L by either Hsp105 or Apg-2 (Fig. 4*E*). Thus, the chaperone-mediated release of PrP^D particles with seeding activity from larger aggregates appears to be more efficient when either the PrP^D n terminus, protease sensitive PrP^D, or possibly other proteins/cofactors, are first removed from PrP^D. Moreover, since the amount of seeding activity from particles released during disaggregation of 22L PrP^D did not significantly vary when centrifuged through layers of 10 to 20% sucrose, the data suggest that the majority of seeding particles were small enough to be retained in sucrose layers ≤10%.

While Hsp105 and Apg-2 facilitated the release of seed particles with similar levels of activity from the protease resistant core samples of 22L, total PrP^D samples disaggregated with Hsp105 had a higher threshold time than samples disaggregated by Apg-2, suggesting that Hsp105 and Apg-2 release different amounts of seed from total PrP^D. To verify this possibility we performed RT-QuIC on dilutions of 22L total PrP^D disaggregated with the help of either Hsp105 (Fig. 5*A*) or Apg-2 (Fig. 5*B*) and analyzed the threshold time at each dilution (Fig. 5*C*). Consistent with a higher number of prion aggregates with seeding activity, lower threshold times for particles released from 22L PrP^D exposed to Apg-2 were

Table 1

Number of positive wells[a]

	None				G/J/Apg-2				G/J/Hsp105			
	Total PrP^D		Protease resistant core		Total PrP^D		Protease resistant core		Total PrP^D		Protease resistant core	
	22L	87V	22L	87V	22L	87V	22L	87V	22L	87V	22L	87V
No spin	8/8	8/8	8/8	8/8	8/8	8/8	8/8	8/8	8/8	8/8	8/8	8/8
10%	0/8	0/8	0/8	0/8	8/8	0/8	8/8	2/8	7/8	0/8	8/8	0/8
15%	0/8	0/8	3/8	0/8	8/8	0/8	8/8	0/8	8/8	0/8	8/8	0/8
20%	0/8	0/8	0/8	2/8	8/8	0/8	8/8	0/8	7/8	0/8	8/8	2/8

Average threshold time (Hr)[b]

	None				G/J/Apg-2				G/J/Hsp105			
	Total PrP^D		Protease resistant core		Total PrP^D		Protease resistant core		Total PrP^D		Protease resistant core	
	22L	87V	22L	87V	22L	87V	22L	87V	22L	87V	22L	87V
No spin	9.6 ± 1.3	23.8 ± 9.5	12.9 ± 4	29.2 ± 16.6	8.1 ± 1.5	24.8 ± 10.2	9 ± 1.7	20.8 ± 7.4	8.6 ± 1.5	18.9 ± 6.2	9.1 ± 1.6	24.8 ± 8.6
10%	N/A	N/A	N/A	N/A	23.8 ± 14.5	N/A	19 ± 7.3	67.3[c]	33 ± 9.6	N/A	19.8 ± 5.9	N/A
15%	N/A	N/A	59.3 ± 8.5	N/A	23.7 ± 13.8	N/A	16.1 ± 6.5	N/A	29.4 ± 10.4	N/A	17.7 ± 7.6	N/A
20%	N/A	N/A	N/A	54[c]	15 ± 6	N/A	26.7 ± 9.3	N/A	36.8 ± 19.9	N/A	26.1 ± 14	66.3[c]

[a] # of Positive Wells/Total Wells.
[b] Threshold set to 2x baseline fluorescence of each well. Number denotes average ± SD in hours (Hr).
[c] Average based on n = 2 wells.

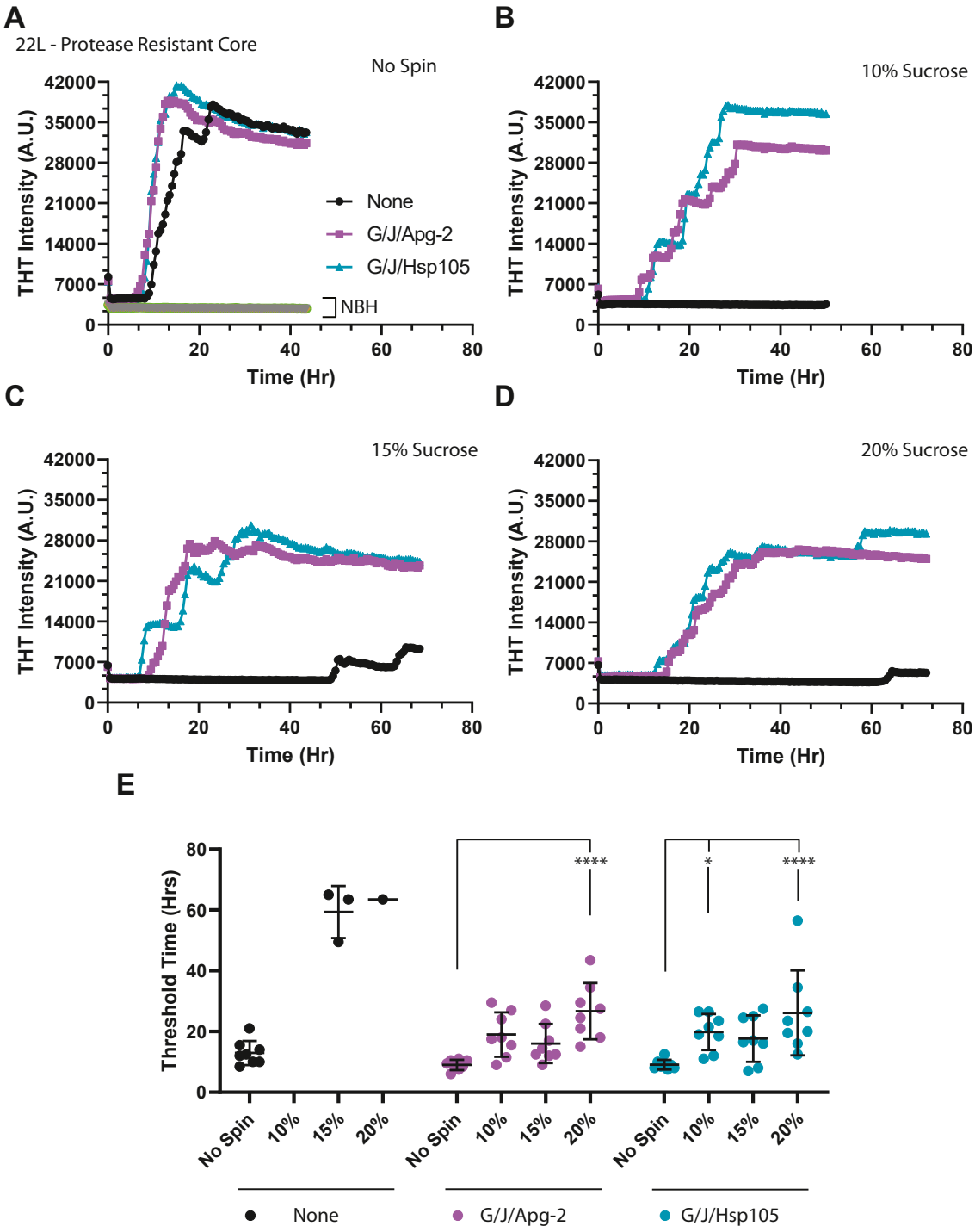

Figure 4. Apg-2 and Hsp105 release similar amounts of seeding particles from the protease resistant core of 22L PrP^D. The protease resistant core of 22L PrP^D was incubated in ATP and an ATP regeneration system for 30 min alone (none, *black lines* and *circles*) or with Grp78, DnaJC1, and either Hsp105 (G/J/Hsp105, *blue lines* and *triangles*) or Apg-2 (G/J/Apg-2, *purple lines* and *squares*). The real-time quaking-induced conversion assay was used to test the seeding activity in samples that were (*A*) not centrifuged (No Spin) as well as the supernatants of samples that were centrifuged over layers of (*B*) 10, (*C*) 15, and (*D*) 20% sucrose. The brackets in (*A*) indicate uninfected, normal brain homogenate (NBH) control samples, that were, or were not, exposed to each chaperone set. The plots shown are based on the average of eight independent samples. *E*, the threshold times in hours (Hrs) was determined as in the legend to Figure 3 with the number of positive wells, average, and standard deviation (None; *black circles*, G/J/Apg-2; *purple circles*, G/J/Hsp105; *blue circles*) for each sample set given in Table 1. Significance was determined using a two-way ANOVA with Tukey's multiple comparisons. p^* = 0.01 to 0.04 and $p^{****} = < 0.0009$.

seen at every dilution when compared to 22L PrP^D exposed to Hsp105 (Fig. 5*C*). Taken together, the data strongly suggest that chaperones facilitate the formation of prion particles with seeding activity by releasing smaller particles from larger aggregates in a manner dependent upon both proteolytic exposure and the cellular chaperones available.

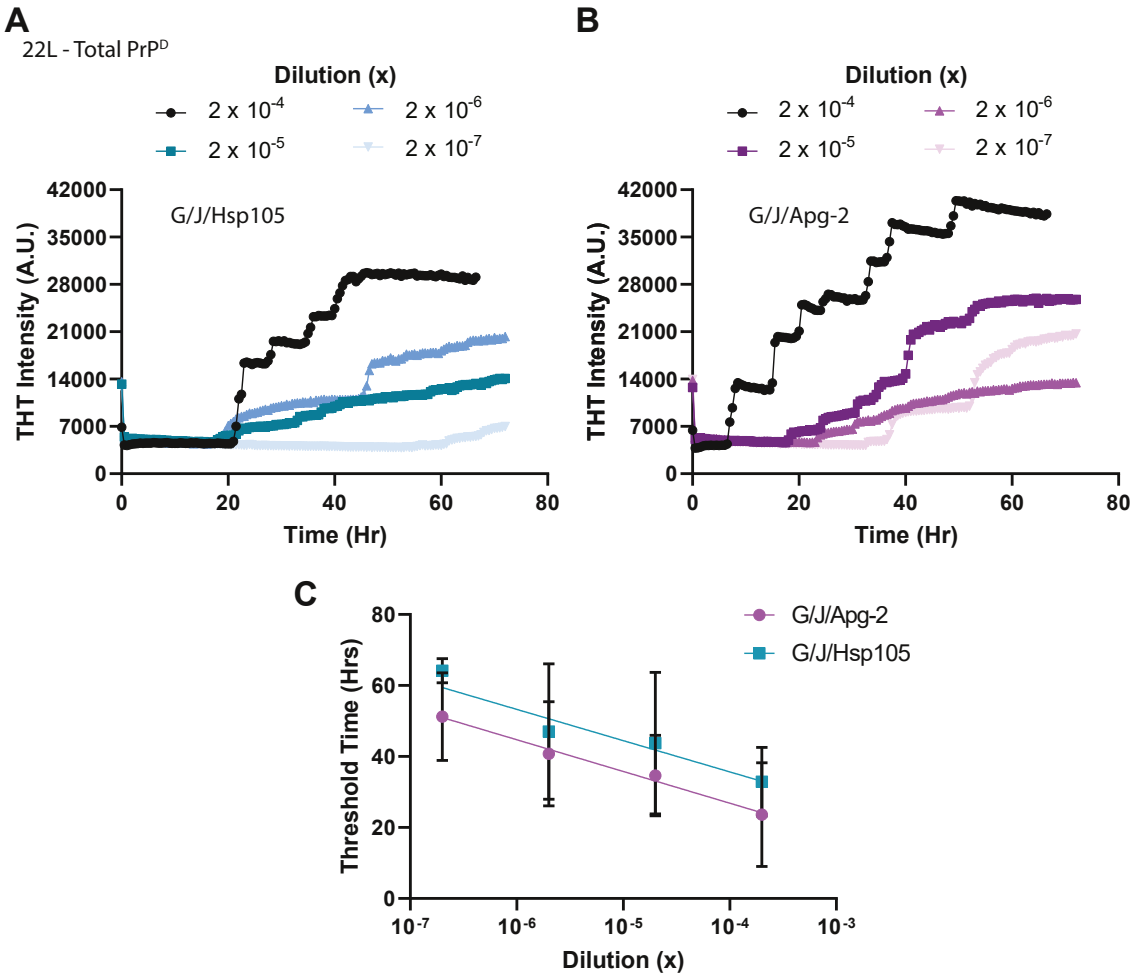

22L Total PrP^D				
Dilution	G/J/Apg-2		G/J/Hsp105	
	AVG ± STDev	# of Wells	AVG ± STDev	# of Wells
2 x 10^{-4}	23.6 ± 14.6	8 / 8	32.9 ± 9.7	7 / 8
2 x 10^{-5}	34.6 ± 11.3	7 / 8	43.8 ± 20	8 / 8
2 x 10^{-6}	40.8 ± 14.7	7 / 8	47 ± 19.1	8 / 8
2 x 10^{-7}	51.3 ± 12.4	8 / 8	64.2 ± 3.4	3 / 8

Figure 5. Grp78 and DnaJC1 in the presence of Apg-2 liberated more seeding particles from 22L total PrP^D than Grp78 and DnaJC1 in the presence of Hsp105. The relative amount of seeding activity produced during disaggregation of 22L total PrP^D exposed to Grp78, DnaJC1, and either (*A*) Hsp105 (G/J/Hsp105) or (*B*) Apg-2 (G/J/Apg-2) was analyzed by real-time quaking-induced conversion across a 1000-fold dilution range (indicated by colored lines as shown in each panel legend). The threshold times in hours (Hrs) was determined for all positive wells across all dilutions. *C*, plot of dilution *versus* average threshold time for samples disaggregated with either Hsp105 (*blue squares* and *lines*) or Apg-2 (*purple circles* and *lines*). All samples were incubated with ATP and an ATP regeneration system. Error bars represent the standard deviation for each point. For each sample set, the number of positive wells and the average ± standard deviation of time in hours to threshold is shown in the table.

Disaggregation of 87V PrP^D facilitated by Hsp105 and Apg-2 does not release particles capable of seeding new PrP^D

Treatment of 87V PrP^D with chaperones also led to the release of prion protein, although the amount released was lower than that from 22L (Fig. 2). In order to test whether there were also fewer PrP^D particles with seeding activity, the supernatants from both chaperone-treated 87V total PrP^D (Fig. 6) and its protease resistant core (Fig. 7) were tested for seeding activity using the RT-QuIC assay. While seeding particles were robustly detected in supernatants of 22L PrP^D samples exposed to chaperones (Figs. 4 and 5), the same was not true of 87V PrP^D. Seeding activity was detected in nonpelleted samples of both 87V total PrP^D (Fig. 6, *A* and *E*, No Spin) and the 87V PrP^D protease resistant core (Fig. 7, *A* and *E*, No Spin). However, while the same concentration of PrP^D was used for 22L and 87V in all assays, the average threshold time was longer in samples of 87V, suggesting that a lower number of the particles released by chaperones had seeding activity (compare Figs. 3*E*

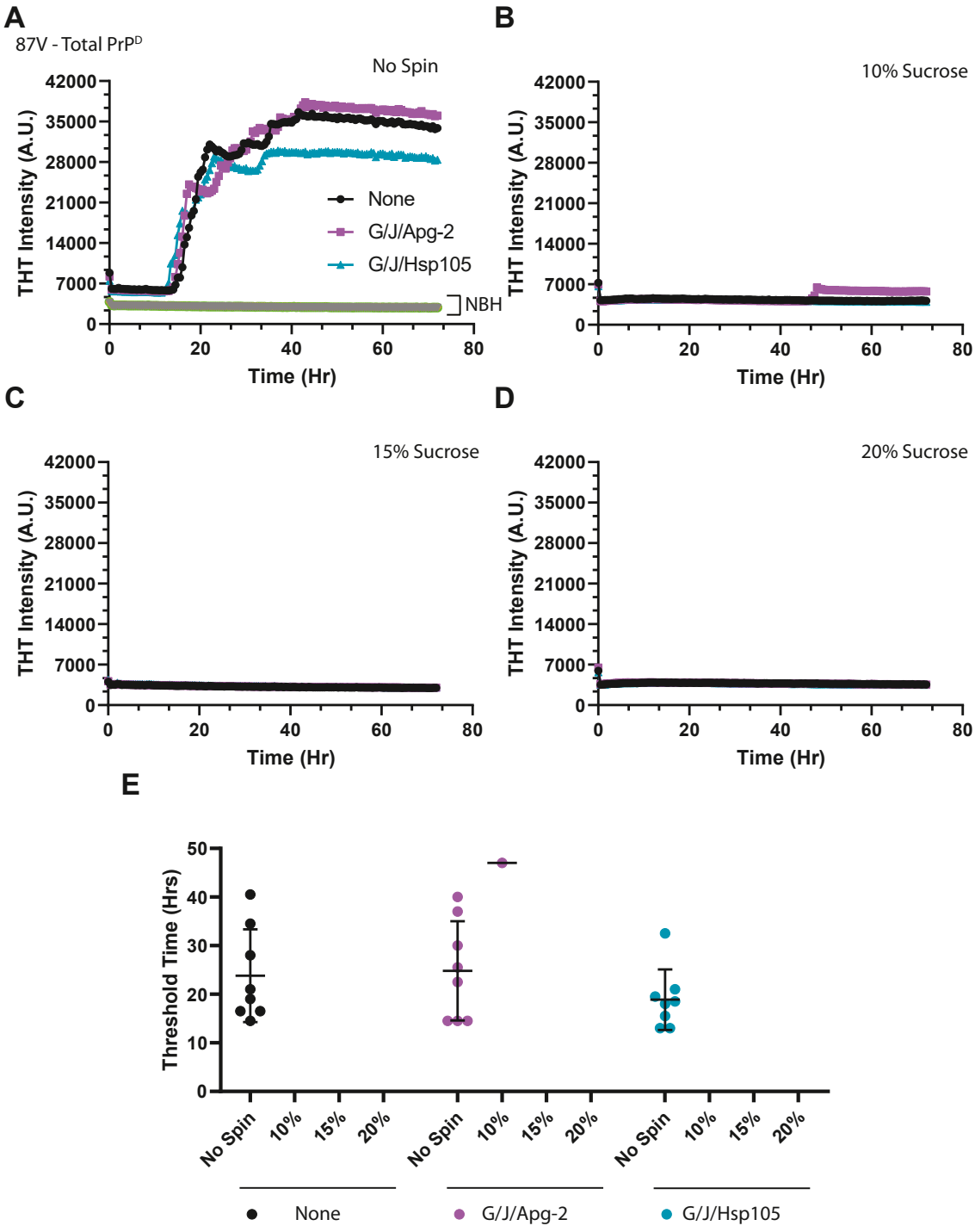

Figure 6. Exposure of total 87V PrP^D to chaperones does not yield prion particles with observable seeding activity. The seeding activity of (*A*) 87V total PrP^D and supernatants produced by centrifugation over (*B*) 10, (*C*) 15, and (*D*) 20% sucrose after incubation with Grp78, DnaJC1, and either Hsp105 (G/J/Hsp105, *blue lines* and *triangles*) or Apg-2 (G/J/Apg-2, *purple lines* and *squares*) was determined *via* real-time quaking-induced conversion. A control sample not exposed to chaperones or centrifuged (none, *black lines* and *circles*) was prepared alongside samples incubated with chaperones. All reactions were carried out in the presence of ATP and an ATP regeneration system for 30 min. The bracket in (*A*) indicates controls for spontaneous prion conversion utilizing normal brain homogenate (NBH) samples that were or were not exposed to each chaperone set. All plots are averages of eight samples. *E*, the plot shows the average threshold times in hours (Hrs) and associated standard deviations (none; *black circles*, G/J/Apg-2; *purple circles*, G/J/Hsp105; *blue circles*) that were calculated for wells that tested positive for seeding activity as defined by crossing a threshold set to two times the baseline. The number of positive wells, average, and standard deviation for each sample set can be seen in Table 1.

and 4*E* to 6*E* and 7*E*). In order to determine the difference in seeding particles between strains, we performed end point dilutions to quantify the seeding activity for total PrP^D and the protease resistant core of both the 22L and 87V stocks used for our experiments. The results showed that 22L PrP^D had about one log more seeding activity than 87V PrP^D (Fig. S3).

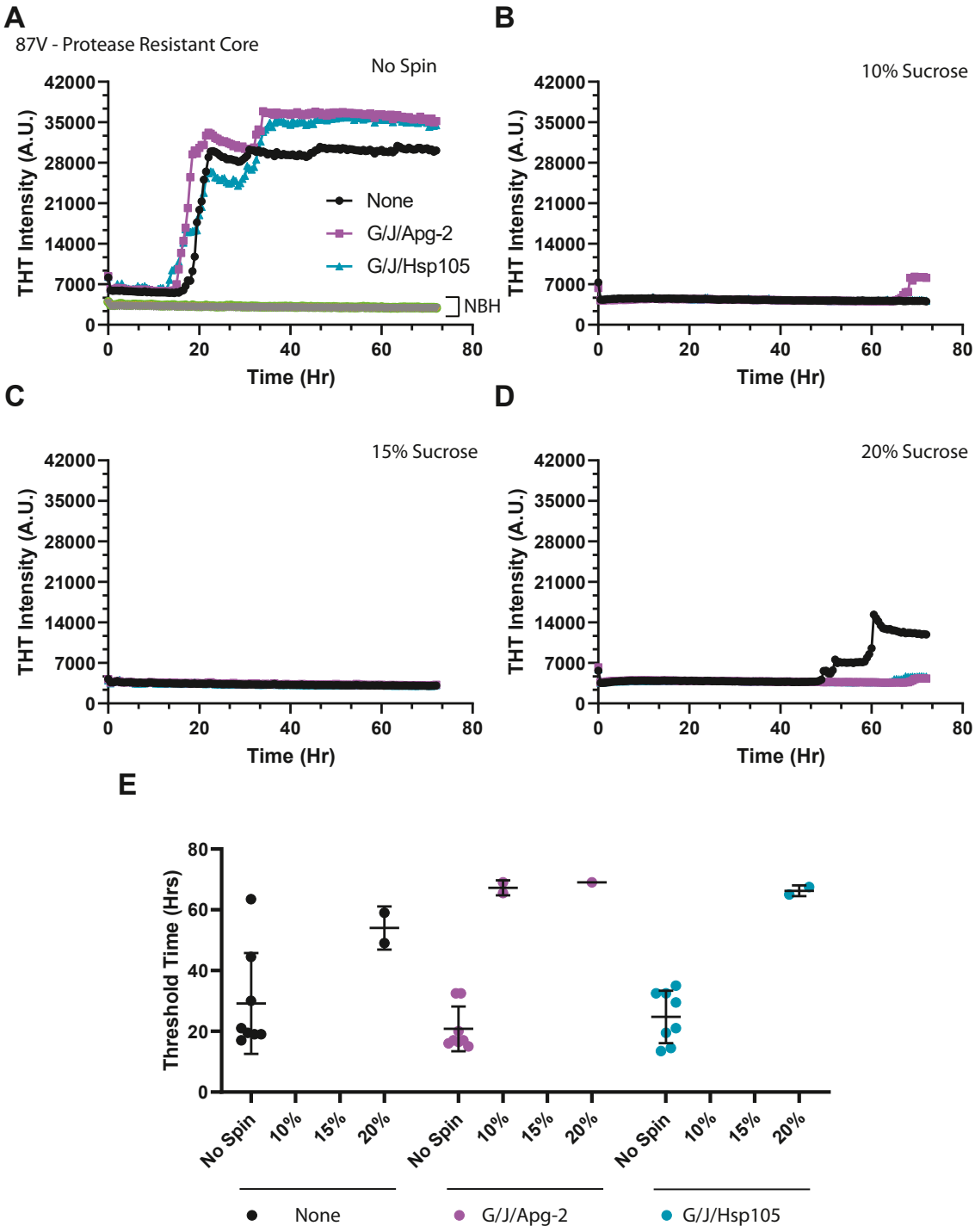

Figure 7. Minimal release of prion seeding activity following the chaperone-mediated disaggregation of the protease resistant core of 87V PrP^D. *A*, The protease resistant core of 87V and the resultant supernatants from centrifugation over (*B*) 10, (*C*) 15, and (*D*) 20% sucrose for samples incubated with Grp78, DnaJC1, and either Hsp105 (G/J/Hsp105, *blue lines* and *triangles*) or Apg-2 (G/J/Apg-2, *purple lines* and *squares*) were tested for seeding activity with real-time quaking-induced conversion. A control sample not exposed to chaperones or centrifuged (none, *black lines* and *circles*) was prepared alongside samples incubated with chaperones. All reactions were carried out in the presence of ATP and an ATP regeneration system for 30 min. The bracket in (*A*) indicates controls for spontaneous prion conversion using normal brain homogenate (NBH) samples that were or were not exposed to each chaperone set. All plots are averages of eight samples regardless of positivity for seeding activity. *E*, the plot shows the average threshold times in hours (Hrs) and associated standard deviations (None; *black circles*, G/J/Apg-2; *purple circles*, G/J/Hsp105; *blue circles*) that were calculated for wells that tested positive for seeding activity as defined by crossing a threshold set to two times the baseline. The number of positive wells, average, and standard deviation for each sample are given in Table 1.

Following centrifugation through 10 to 20% sucrose, a few wells tested positive after 50 h or more in samples of the protease resistant core of 87V PrP^D without chaperones added (Fig. 7, *D* and *E*). This was similar to what was observed with 22L PrP^D (Fig. 4) and suggests that, regardless of the prion strain, protease treatment alone may free a small number of

seeding particles from larger aggregates. However, little or no seeding activity was detected in supernatants from either chaperone-treated 87V total PrP^D (Fig. 6, *B–E*, Table 1) or the chaperone-treated 87V PrP^D protease resistant core (Fig. 7, *B–E*, Table 1). Since 87V possesses around one log less seeding activity than 22L (Fig. S3), we considered that 87V PrP^D seeding activity might be detectable in less diluted samples. We thus retested supernatants from 87V total PrP^D and its protease resistant core that had been incubated with Grp78/DnaJC1 and Apg-2 at 10- and 100-times higher concentrations using the RT-QuIC assay. Once again, we found no trace of seeding activity (Fig. S4), suggesting that the one log difference in seeding activity between 22L and 87V PrP^D is insufficient to explain the difference in seeding activity in PrP^D particles released following incubation with chaperones. Thus, as opposed to 22L PrP^D, the chaperone-mediated disaggregation of 87V PrP^D did not result in the release of a detectable amount of PrP^D particles with seeding activity, indicating that the amount and propensity to release small aggregates with seeding activity by chaperones is prion strain specific. Overall, our data suggest not only that the aggregates released from 87V PrP^D by chaperones are unable to seed new prion formation, but also that there is a fundamental difference in the way chaperones interact with 87V PrP^D when compared to 22L PrP^D.

Grp78 and DnaJC1 alone release 22L PrP^D particles with seeding activity

We have previously shown that Grp78 and DnaJC1 alone were able to disaggregate a small fraction of 22L, but not 87V, PrP^D (28). Thus, we wanted to ascertain whether the PrP^D particles released by the activity of Grp78 and DnaJC1 alone were able to seed new PrP^D formation. We therefore exposed 22L PrP^D that had, or had not, been pretreated with proteases to Grp78 and DnaJC1 for 30 min before centrifuging all samples over a 10% sucrose layer and testing the supernatant for seeding activity using the RT-QuIC assay (Fig. 8). Interestingly, seeding particles of 22L were released from both total PrP^D and its protease resistant core following incubation with Grp78 and DnaJC1. Based on threshold times, 54.3 h for 22L total PrP^D and 39.6 h for its protease resistant core, the amount of seeding activity appeared to be greater in particles released from the protease resistant core. The threshold times of total PrP^D and protease resistant core samples were almost twice as long as the threshold times observed with Hsp105 or Apg-2 present (Figs. 3 and 4). By using the dilution curves shown in Figure 7*C*, the difference in seeding activity can be approximated to be about two orders of magnitude lower in the absence of Hsp110s. Thus, while the data indicate that Hsp110s facilitate the Grp78-mediated disaggregation and release of seeding particles, the activity of Grp78/DnaJC1 alone can still liberate seeding particles from PrP^D and may contribute to prion propagation independently of the presence of Hsp110s.

Chaperone disaggregated 87V PrP^D particles are less PK resistant than chaperone disaggregated 22L PrP^D particles

Both Hsp105 and Apg-2 facilitated the disassembly of 22L and 87V PrP^D, but significant seeding activity was only

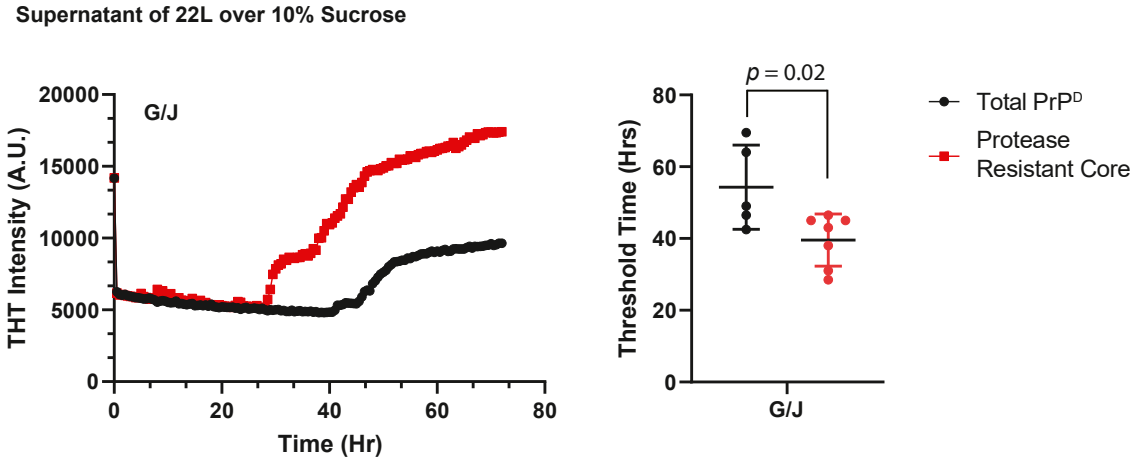

G/J		
22L	Average ± STDev	# of Wells
Total PrP^D	54.3 ± 11.9	5/8
Protease Resistant Core	39.6 ± 7.3	7/8

Figure 8. 22L PrP^D seeding particles are released following incubation with the chaperones Grp78 and DnaJC1. *Left* panel samples of 22L total PrP^D (*black lines* and *circles*) and its protease resistant core (*red lines* and *squares*) were incubated with Grp78 and DnaJC1 (G/J) for 30 min in the presence of ATP and an ATP regeneration system. All samples were spun over 10% sucrose and their supernatants were tested for seeding activity using real-time quaking-induced conversion. A total of eight wells for each sample were averaged and plotted. The average and standard deviation threshold times in hours (Hrs) for positive wells for total PrP^D (*black circles*) and for the protease resistant core (*red circles*) are plotted in the *right* panel. The number of positive wells as well as the values for average threshold time and standard deviation are given in the table.

observed in particles liberated from 22L PrP^D. This could be explained by the chaperones either not solubilizing 87V PrP^D efficiently or by unfolding it enough to destroy its conformational properties, thus abolishing its seeding activity. We therefore determined the degree to which disaggregated 22L and 87V PrP^D were PK resistant (Fig. 9). Total PrP^D and the protease resistant core from both strains was incubated with Grp78, DnaJC1, and Apg-2 for 30 min, with ATP and an ATP regeneration system, before samples were centrifuged over 10% sucrose. The supernatants, which contained prion protein liberated from larger aggregates, were split and one half treated with 10 μg/ml PK while the other half was not. Immunoblot results (Fig. 9*A*) and subsequent quantification (Fig. 9*B*) show that, for both total PrP^D and its protease resistant core, a much larger percentage of chaperone released 22L PrP^D is PK resistant when compared with 87V PrP^D. Compared to untreated PrP^D, about 55 and 1%, respectively, of chaperone treated 22L and 87V total PrP^D remained PK resistant, while 55 and 10%, respectively, of the chaperone treated protease resistant core of 22L and 87V PrP^D also remained PK resistant. The results are consistent with 87V PrP^D released by chaperones likely being unfolded and at least partially conformationally altered, thus losing its ability to seed new PrP^D formation.

Discussion

In this work, we investigated the ability of Grp78, DnaJC1, and two members of the Hsp110 chaperone family, Hsp105 and Apg-2, to disassemble and disrupt the properties of PrP^D from two different mouse prion strains, 22L and 87V. We demonstrate that, for both strains, Grp78/DnaJC1 in combination with either Hsp105 or Apg-2 reduces the PK resistance of PrP^D at neutral pH (Fig. 1) and disaggregates 10 to 30% of PrP^D within 30 min (Fig. 2). Previously, we had demonstrated that the ability of Grp78/DnaJC1 and Hsp90/Stip1 to reduce PrP^D PK resistance was dependent upon low pH induced destabilization of PrP^D, leading to an observable disaggregation of only ~1% of the 22L PrP^D protease resistant core (28). However, all of the chaperone-mediated disaggregation reactions in the current manuscript were done at neutral pH and were thus independent of low pH induced destabilization of PrP^D. Therefore, while our data show that multiple different chaperone combinations can disaggregate PrP^D, the efficiency of that disaggregation is likely dependent upon a combination of strain, chaperone set, and environmental conditions. This suggests that the disassembly of prion aggregates by the cell may vary greatly depending upon the available chaperones in different cell types as well as the cellular microenvironment where PrP^D is made and/or accumulates.

The 22L PrP^D liberated by Grp78, DnaJC1, and the Hsp110s was mostly protease resistant and possessed seeding activity, both characteristic properties of infectious PrP^D (2). Seeding activity for 22L PrP^D was observed under every condition with every combination of chaperone tested, though the amount of seeding activity varied between sample set. In general, more particles with seeding activity were released from the protease resistant core of 22L PrP^D regardless of chaperone set, indicating that predigestion with proteases actually increased the efficiency of chaperone-mediated fragmentation. Predigestion with proteases may clear away PrP^C, partially converted PrP^D, protease sensitive PrP^D (57, 58), the protease sensitive n

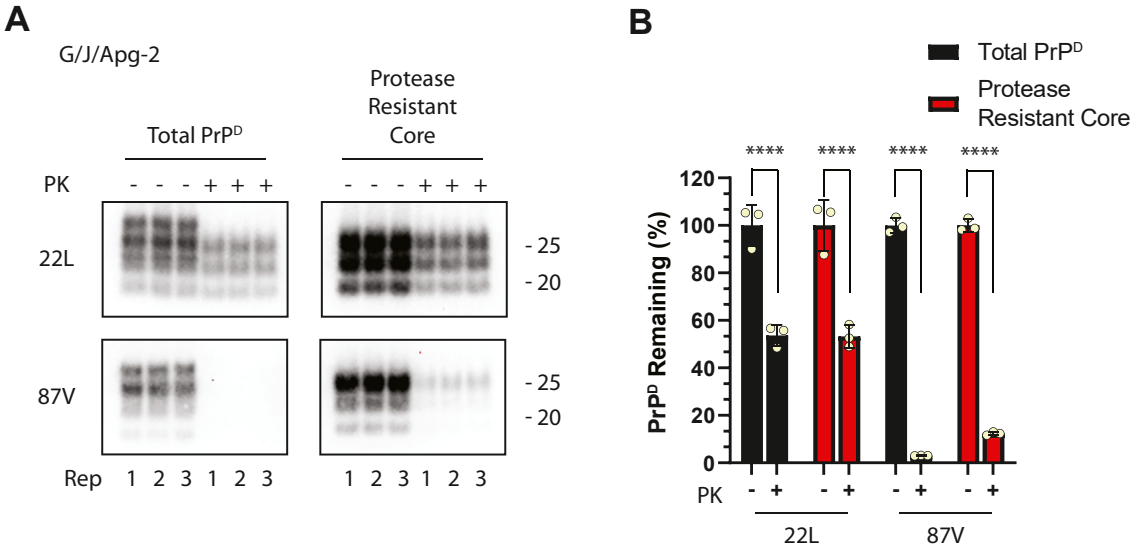

Figure 9. PrP^D particles liberated from 22L PrP^D aggregates by chaperones are more protease resistant than PrP^D particles liberated from 87V. PrP^D particles liberated following incubation with Grp78/DnaJC1 and Apg-2 (G/J/Apg-2) were tested for resistance to PK. After disaggregation, samples were centrifuged over 10% sucrose and supernatants were, or were not, incubated with PK for 1 h. *A*, immunoblot analysis of supernatant samples. All blots were probed with the anti-PrP mouse monoclonal antibody 6D11. Molecular mass markers for 25 kDa (*upper* marker) and 20 kDa (*lower* marker) are shown to the right of each blot. 22L, *upper* blots; 87V, *lower blots*; Total PrP^D, *left* blots; Protease resistant core, right blots; (*B*) The average percentage of PrP^D remaining after PK treatment for total PrP^D (*black bars*) and its protease resistant core (*red bars*) was calculated and is plotted as shown. Percentages were calculated by normalization to samples that were incubated with G/J/Apg-2 but not PK treated. Individual values are shown as *yellow circles*. All samples were incubated with ATP and an ATP regeneration system. Data were calculated from n = 3 replicates (Rep) for each time point shown and are given as mean ± standard deviation. A one-way ANOVA with Tukey's multiple comparisons test was used to determine significance. $p^{****} = < 0.0009$. PK, proteinase K.

terminus of the prion protein (59), or possibly other proteins. If any of these factors help to stabilize aggregates of 22L and/or block chaperone binding sites, their removal would be expected to increase seeding activity, which is what we observed when comparing prion seeding activity released from total 22L PrP^D to that released from its protease resistant core.

Both members of the Hsp110 chaperone family in combination with Grp78 facilitated the release of 22L PrP^D particles with seeding activity. Since both Hsp110s liberated aggregates with similar amounts of seeding activity from the protease resistant core of 22L, it is unlikely that there is a difference either in the ability of Hsp105 and Apg-2 to disrupt the infectious properties of 22L or in their overall ability to remove seeds from larger aggregates. However, when samples were not pretreated with proteases (*i.e.* total PrP^D), Apg-2 liberated seeding particles with significantly more activity than Hsp105. It is possible that differences in the activity of seeding particles released by different chaperones from aggregates that were not pretreated with PK are the result of differences in the exposure of sites where conversion occurs. These differences could be explained by Hsp105 having a higher affinity for proteins and/or nonseeding particles of prion protein, such as PrP^C or partially converted PrP^D, that may still be present in aggregates of total PrP^D (15, 37). Apg-2 may simply be better at directly exposing active conversion sites while Hsp105 requires the removal of other factors to be effective. A higher affinity of Hsp105 for protease-sensitive components of PrP^D could lead to less Hsp105 being available to bind to and release PrP^D seeding particles.

Unlike 22L PrP^D, treatment of 87V PrP^D with chaperones led to the release of particles with no detectable seeding activity that were also much less resistant to PK. Thus, prion protein liberated from aggregates of 87V PrP^D have less of the characteristic properties of infectious prions. This suggests that the chaperones are either destroying the infectious conformational properties of 87V PrP^D during disaggregation or removing nonseeding particles, such as PrP^C or partially converted PrP^D. Previous work has shown that protease sensitive material can be buried inside large aggregates of both 22L and 87V PrP^D (15), and that these protease sensitive molecules may be released during disaggregation of both total PrP^D and its protease resistant core. In the current article as well as in previous work (28), chaperones have also been found to alter the structural properties of 22L and 87V PrP^D, as indicated by a loss of protease resistance. Failure to observe seeding activity or protease resistance in 87V PrP^D particles released by chaperone activity indicates that there are strain-specific structural differences between 22L and 87V that either prevent chaperones from liberating seeding particles of 87V PrP^D or that allow them to fully disrupt their conformational properties.

The progression of prion disease is faster in mice infected with 22L compared to mice infected with 87V while multiple cell lines can support 22L, but not 87V, prion infection (60). We have previously suggested that the ability of the cell to more rapidly degrade 87V PrP^D compared to 22L PrP^D could in part explain the inability of 87V prions to infect cells as well as the more rapid disease induced by 22L prions (36). Given their lack of seeding activity and increase in protease sensitivity, the current data suggest that the particles released from 87V PrP^D by chaperones may also be, at the very least, not as infectious as those liberated from 22L PrP^D. This could significantly impact the ability of 87V to spread from cell-to-cell and establish productive prion infection both *in vivo* and *in vitro*. It is important to note, however, that there are likely multiple other ways for chaperones to promote the spread of 87V. Different chaperone sets than those used in our study could interact with 87V PrP^D to release particles that can seed new prion formation. In addition, chaperone induced structural destabilization within aggregates of 87V PrP^D could create weak points allowing them to be fragmented by cellular proteases or shearing forces generated by cellular processes, such as changes in membrane dynamics during endocytosis or cell division. Finally, even if the material liberated from 87V by chaperones lacked the ability to seed new PrP^D, the slow disaggregation of 87V PrP^D could make the core of the aggregate small enough to move between cells or allow chaperones to clear away unconverted material and other proteins from 87V PrP^D that may block conversion sites.

We observed that the Hsp110 chaperones facilitated the ability of Grp78 and DnaJC1 to unfold and disassemble PrP^D. However, chaperone-mediated PrP^D disaggregation also led to the release of PrP^D particles that could seed new PrP^D formation, potentially promoting prion replication and spread. What determines whether Hsp110 activity facilitates or disrupts the formation of seeding particles may be dependent upon the concentration of Hsp110, as suggested by a study in *Drosophila* which found that overexpressing Apg-2 reduced the amount of PrP^D seeding particles (50). Thus, Hsp110 chaperones may play a dual role in prion biology with diametrically opposed outcomes: disassembly of PrP^D to destroy infectious prions and release of PrP^D seeding particles to enhance prion replication. Chaperones play a similar role in the propagation of yeast prions as they possess a dual activity where they situationally facilitate (61) or disrupt (62, 63) the formation and accumulation of yeast prions. The data in the current article are consistent with this and suggest that chaperones could play a role in the different disease progressions observed in 22L and 87V. In a similar manner to yeast, 22L and 87V PrP^D may have different susceptibilities to structural destabilization by the same chaperones, with the threshold for destabilization potentially dependent upon the chaperone concentration. Thus, a dose-dependent chaperone activity that liberates PrP^D particles with seeding activity from 22L, but not 87V, PrP^D aggregates, would only promote prion replication and spread of 22L prions. By contrast, the release of fewer particles with seeding activity from 87V PrP^D aggregates could be protective by favoring, over time, prion degradation over prion replication leading to (1) an inability of PrP^D formation in cells *in vitro* to outpace degradation and (2) a slower spread of 87V prions *in vivo*. Further study of chaperone-prion interactions may help us to not only understand how chaperone imbalance may foster prion accumulation but also how chaperone systems may be tuned to create effective treatments for prion disease.

Experimental procedures

Prion propagation and animal care

This study was carried out in accordance with the *Guide for the Care and Use of Laboratory Animals* of the National Institutes of Health (64). The Rocky Mountain Laboratories Animal Care and Use Committee reviewed and approved all protocols used for animal experiments (protocol number 2021–023-E). Both 22L and 87V were propagated as described previously in C57BL/10 and VMDK mice, respectively (65). Mice were monitored until they showed unambiguous signs of prion disease including altered grooming and nesting habits, ataxia, and altered posture. Mice were then euthanized by isoflurane overdose followed by cervical dislocation and brains harvested and stored at −80 °C until use.

Brain homogenization and PTA precipitation of PrP^D

Brains from mice infected with either 22L or 87V were suspended in PBS to a concentration of 10% (wt/vol) before being homogenized with a Mini-BeadBeater-8 instrument (Biospec) and clarified *via* centrifugation at 500*g* for 5 min (min), as described previously (36). Brain homogenates were then mixed with sarkosyl to 2% by diluting the clarified homogenates 1:1 with 4% sarkosyl. Homogenates were vortexed and incubated at 37 °C for 30 min before being mixed with benzonase (Sigma-Aldrich) to 0.05 Units/μL and magnesium chloride to 1 mM. The solution of benzonase and brain homogenate was mixed briefly before being incubated for 45 min at 37 °C. After benzonase digestion, brain homogenates were centrifuged at 5000g for 5 min. Half of each brain homogenate supernatant sample was then treated with 50 μg/ml proteinase K (Novagen) for 1 h at 37 °C while the other half was not. The protease inhibitor Pefabloc (Sigma-Aldrich) was then added to both samples to 5 mM. Sodium phosphotungstic acid hydrate (PTA, Sigma-Aldrich) was added to a final concentration of 3.2 μg/ml and the homogenate incubated for 1.5 h at 37 °C. PTA treated homogenates that were or were not PK treated were then centrifuged at 16000*g* for 30 min at room temperature in order to pellet PrP^D. PTA was removed from pelleted material with a wash in PBS containing 0.1 M EDTA. Pellets were vortexed and incubated at 37 °C for 30 min before being centrifuged again at 16000*g* for 30 min at room temperature. The resulting PrP^D pellets were then resuspended in PBS, mixed with glycerol to 15%, snap frozen, and stored at −80 °C until use.

Protein expression and purification

Grp78, DnJC1, Hsp105, and Apg-2 were expressed in *Escherichia coli* and purified at RML by methods outlined in previous work (28). The pET-14b plasmid was engineered by GenScript to express the genes for Grp78, DnaJC1, Hsp105, and Apg-2 with a cleavable His6x affinity tag. The His6x tag on WT mouse genes for Grp78, Hsp105, and Apg-2 was attached to proteins *via* a cleavable Sumo protein tag while the luminal domain of DnaJC1 from amino acids 46 to 148, referred to as DnaJC1 throughout this work, was expressed behind a thrombin cleavable His6x tag. Plasmids were transformed into *E. coli* BL21(DE3) competent cells (Thermo Fisher Scientific) by heat shock at 42 °C before being plated on ampicillin antibiotic Lysogeny Broth agar plates. Colonies were picked and grown at 37 °C and 200 rpm overnight before being diluted 1:1000 and regrown at 37 °C and 200 rpm to an A_{600} of 0.6 for Grp78 and DnaJC1 and an A_{600} of 0.7 for Hsp105 and Apg-2. Expression of all genes was induced with 0.4 mM of isopropyl-1-thio-β-D-galactopyranoside (Sigma-Aldrich). All proteins were expressed for 3 to 4 h at 37 °C before *E. coli* was pelleted with a 5000*g* spin at 4 °C.

Purification of Grp78, DnaJC1, Hsp105, and Apg-2 was performed similarly to previous work (28). In short, *E. coli* pellets were resuspended in phosphate lysis buffer (50 mM NaH_2PO_4 pH 8.0, 300 mM NaCl, 10 mM imidazole, 5 mM β-mercaptoethanol, 10% sucrose, containing 2x cOmplete Mini EDTA-free protease inhibitor cocktail (Sigma-Aldrich)) and passaged through a French press cell disrupter (Thermo Fisher Scientific) three times to lyse cells. Cell lysates were centrifuged at 35000*g* for 30 min, and the clarified lysates were then run over an Ni-NTA Superflow resin (Qiagen). The Ni-NTA column was rinsed with phosphate wash buffer (25 mM NaH_2PO_4 pH 8.0, 300 mM NaCl, 20 mM imidazole, and 5 mM β-mercaptoethanol), and protein was eluted with a series of step washes containing 25 to 400 mM imidazole. Fractions containing target proteins were pooled and their His6x tags were removed with either SUMO protease (Thermo Fisher Scientific) or thrombin (Thermo Fisher Scientific). Protein was rerun over an Ni-NTA column to remove affinity tags before being dialyzed into ion exchange column loading buffer (50 mM Tris–HCl pH 7.4, 25 mM NaCl, 0.1 mM EDTA, and 5 mM β-mercaptoethanol) and run over a HiTrap Q HP column (Cytiva). Proteins were eluted over a linear gradient from 25 to 1000 mM NaCl and purity was determined *via* SDS-PAGE. If protein was less than 99% pure it was either rerun over a Q column or separated from contaminants over a Superdex size-exclusion column (Cytiva) run with wash buffer (50 mM Tris–HCl pH 7.4, 150 mM KCl, 0.05 mM EDTA, and 2 mM DTT). Once protein was ≥99% pure fractions were pooled, concentrated, and buffer exchanged into storage buffer (50 mM Tris–HCl pH 7.4, 150 mM KCl, 0.05 mM EDTA, 15% glycerol, and 2 mM DTT) using an Amicon Ultra spin concentrator (Millipore). Samples were snap frozen and stored at −80 °C until use.

Chaperone mediated disaggregation and protease resistance assays

PTA precipitated 22L and 87V PrP^D that was or was not PK treated prior to precipitation was diluted to 0.1 μM in disaggregation buffer (50 mM Hepes pH 7.4, 150 mM KOAc, 10 mM $MgOAc_2$, and 2 mM DTT) containing 2 mM ATP (Sigma-Aldrich), an ATP regeneration system, and chaperones. The negative control sample was the same except that no chaperones were added. The ATP regeneration system was composed of 0.25 μM creatine kinase (Sigma-Aldrich) and 2 mM creatine phosphate (Sigma-Aldrich) (15, 28).

Combinations of chaperones are indicated in each experiment but the concentrations for Grp78, DnaJC1, Hsp105, and Apg-2 were 2, 1, 0.5, and 0.5 μM, respectively. PrP^D from both strains was incubated with and without chaperones for 30 min at 37 °C in an Eppendorf ThermoMixer C with shaking at 300 rpm. Samples were then mixed 1:1 with disaggregation buffer before an aliquot was removed for use in the RT-QuIC assay. Samples were then split and one half was treated with PK at 10 μg/ml and incubated at 37 °C for 1 h while the other half was centrifuged over 10, 15, and 20% sucrose at 18,300*g* in a F301.5 Beckman rotor at 4 °C for 30 min. Supernatants were removed and further split for analysis with small aliquots removed for later testing with RT-QuIC and detection of PrP^D. A portion of the supernatant was removed and digested with PK (10 μg/ml) at 37 °C for 1 h. Pellets were resuspended in 2x NuPAGE sample buffer while PK treated samples were mixed with Pefabloc to 5 mM and incubated for 10 min at room temperature to inactivate PK. Samples not destined for RT-QuIC that were or were not PK treated were mixed with 4x NuPAGE sample buffer (Novex) to a final concentration of 1.5x before being heated at 95 °C for 5 min, spun down, vortexed, snap frozen, and stored at −80 °C until use. Samples destined for RT-QuIC analysis were aliquoted, snap frozen, and stored at −80 °C until use.

SDS-PAGE and Western blots

Gels and blots were prepared as described previously (28). In brief, frozen samples in NuPAGE sample buffer were thawed heated to 95 °C for 5 min, spun down briefly, and then vortexed before being run over 10% Bis-Tris gels for ∼3 h at a constant voltage of 75 V. Gel contents was transferred to polyvinylidene difluoride (EMD Millipore) Immobilon-P membranes at a constant voltage of 34 V overnight in a NuPAGE Novex gel system. After transfer, membranes were incubated in 1xTBST (10 mM Tris–HCl (pH 8.0), 150 mM NaCl, and 0.05% Tween 20) containing 5% powdered milk for 1 h to block the membrane prior to antibody exposure. After rigorous washing, membranes were probed with the 6D11 primary antibody (BioLegends, antibody epitope to PrP^C residues 93–109) diluted 1:10,000 in TBST before being incubated for 1.5 h. Membranes were rigorously washed in 1x TBST before being probed with a horseradish peroxidase-conjugated sheep anti-mouse secondary antibody (GE Amersham) at a 1:50,000 dilution. After a 1 h incubation, membranes were rinsed heavily in 1xTBST and developed with the ECL Plus reagent (GE HealthCare Life Sciences). Membranes were then imaged on an iBright gel imager (Thermo Fisher Scientific).

RT-QuIC assay for PrP^D seeding activity

RT-QuIC assays for seeding activity were set up similarly to previous work (66). Samples to be tested for seeding activity were diluted 1:100 in 1xPBS containing 0.1% SDS before being diluted 1:50 into 0.1 ml reaction solution composed of 1xPBS supplemented with 1 mM EDTA, 10 nM thioflavin T (THT), and 0.1 mg/ml of *E. coli* derived and purified recombinant hamster PrP ($rPrP^{-sen}$, hamster PrP residues 90–231). Reaction solutions were placed into wells of a 96-well Nunc optical bottom plate (Thermo Fisher Scientific) and sealed with polyolefin tape (Thermo Fisher Scientific). Plates were placed into a CLARIOstar plate reader (BMG) heated to 50 °C and fluorescence from THT was recorded with excitation and emission at 450 and 480 nm, respectively. Samples were shaken at 700 rpm for 1 min, allowed to rest for 1 min, and then readings were taken for 1 min. Fluorescence was recorded every 3 min for 40 to 72 h. Samples were considered positive for seeding activity if their THT fluorescence rose above a threshold set to two times the background THT fluorescence in each well. The time it takes for THT to rise above threshold directly correlates with the number of seeding particles/conversion sites (67). Thus, threshold time was used as a comparative metric for seeding activity throughout this work. The percentage of false positives induced by normal brain homogenate across all datasets was 1 to 2%. All false positives occurred after the 65 h time point. Data were analyzed in Excel (Microsoft) for threshold time and averages, deviations, and plots were developed in Graphpad Prism Software (8.0.2; https://www.graphpad.com/).

Blot quantification and data analysis

PrP^D gel bands were quantified using the "Segment Analysis" tool in Un-Scan-IT software (version 7.1; Silk Scientific Corporation; https://www.silkscientific.com/) to sum all pixels in analysis regions. Background values derived from regions near the bands being quantified were subtracted from the total PrP^D pixels as described previously (28). Pixel sum values were then divided by the average pixel sum of PrP^D that was either not exposed to chaperones or was pelleted in order to respectively calculate changes in PK resistance and the amount of prion protein liberated by chaperones. Average normalized pixel sums were then converted to a percentage by multiplying values by 100. For all plots, data are shown as an average with error bars representing the standard deviations and individual points overlaid. For blot data, averages are calculated from three replicates while data from RT-QuIC assays is calculated from different numbers of replicates, which are indicated in the accompanying tables. Graphpad Prism Software (version 8.0.2; https://www.graphpad.com/) was used for data management and statistical calculations. The type of statistical test used is indicated in the Figure Legends. The asterisks in figures represent *p*-values within specific ranges with p^* = 0.01 to 0.04, p^{**} = 0.005 to 0.009, p^{***} = 0.001 to 0.004, and p^{****} = < 0.0009.

Data availability

Data shared upon request.

Supporting information—This article contains supporting information.

Data analysis—All values are expressed as the mean ± SD

Acknowledgments—We thank Dr Brent Race and Dr Byron Caughey for insightful discussion and commentary on the manuscript. In

addition, Dr Brent Race generously provided many of the noninfected mouse brains used in this work and we are thankful for his support of this project. We would also like to thank Andy Hughson for helpful discussion on developing and running RT-QuIC assays as well as for providing the RT-QuIC substrate.

Author contributions—D. W. S. and S. A. P. writing–review and editing; D. W. S. and S. A. P. conceptualization; D. W. S. validation; D. W. S. methodology; D. W. S. investigation; D. W. S. data curation; D. W. S. formal analysis; D. W. S. visualization; D. W. S. writing–original draft; S. A. P. funding acquisition.

Funding and additional information—This research was supported by a grant from the National Institutes of Health, National Institute of Allergy and Infectious Diseases, Division of Intramural Research. The content is solely the responsibility of the authors and does not necessarily represent the official views of the National Institutes of Health.

Conflict of interest—The authors declare that they have no conflicts of interest with the contents of this article.

Abbreviations—The abbreviations used are: PK, proteinase K; PTA, phosphotungstic acid hydrate; RT-QuIC, real-time quaking-induced conversion; TBST, 10 mM Tris–HCl (pH 8.0), 150 mM NaCl, and 0.05% Tween 20; THT, thioflavin T.

References

1. Colby, D. W., and Prusiner, S. B. (2011) Prions. *Cold Spring Harbor Perspect. Biol.* **3**, a006833
2. Gill, A. C., and Castle, A. R. (2018) The cellular and pathologic prion protein. In *Handbook of Clinical Neurology*, Elsevier: 21–44
3. Hoyt, F., Alam, P., Artikis, E., Schwartz, C. L., Hughson, A. G., Race, B., *et al.* (2022) Cryo-EM of prion strains from the same genotype of host identifies conformational determinants. *PLoS Pathog.* **18**, e1010947
4. Atarashi, R., Sim, V. L., Nishida, N., Caughey, B., and Katamine, S. (2006) Prion strain-dependent differences in conversion of mutant prion proteins in cell culture. *J. Virol.* **80**, 7854–7862
5. Bessen, R. A., Kocisko, D. A., Raymond, G. J., Nandan, S., Lansbury, P. T., and Caughey, B. (1995) Non-genetic propagation of strain-specific properties of scrapie prion protein. *Nature* **375**, 698–700
6. Legname, G., Nguyen, H. O. B., Peretz, D., Cohen, F. E., DeArmond, S. J., and Prusiner, S. B. (2006) Continuum of prion protein structures enciphers a multitude of prion isolate-specified phenotypes. *Proc. Natl. Acad. Sci.* **103**, 19105–19110
7. Bessen, R. A., and Marsh, R. F. (1992) Identification of two biologically distinct strains of transmissible mink encephalopathy in hamsters. *J. Gen. Virol.* **73**, 329–334
8. Morales, R., Abid, K., and Soto, C. (2007) The prion strain phenomenon: molecular basis and unprecedented features. *Biochim. Biophys. Acta (BBA)-Molecular Basis Dis.* **1772**, 681–691
9. Yim, Y.-I., Park, B. C., Yadavalli, R., Zhao, X., Eisenberg, E., and Greene, L. E. (2015) The multivesicular body is the major internal site of prion conversion. *J. Cel. Sci.* **128**, 1434–1443
10. Goold, R., Rabbanian, S., Sutton, L., Andre, R., Arora, P., Moonga, J., *et al.* (2011) Rapid cell-surface prion protein conversion revealed using a novel cell system. *Nat. Commun.* **2**, 1–11
11. Arnold, J. E., Tipler, C., Laszlo, L., Hope, J., Landon, M., and Mayer, R. J. (1995) The abnormal isoform of the prion protein accumulates in late-endosome-like organelles in scrapie-infected mouse brain. *J. Pathol.* **176**, 403–411
12. Caughey, B., and Raymond, G. J. (1991) The scrapie-associated form of PrP is made from a cell surface precursor that is both protease- and phospholipase-sensitive. *J. Biol. Chem.* **266**, 18217–18223
13. Shorter, J. (2011) The mammalian disaggregase machinery: Hsp110 synergizes with Hsp70 and Hsp40 to catalyze protein disaggregation and reactivation in a cell-free system. *PLoS One* **6**, e26319
14. Tiwari, S., Fauvet, B., Assenza, S., De Los Rios, P., and Goloubinoff, P. (2023) A fluorescent multi-domain protein reveals the unfolding mechanism of Hsp70. *Nat. Chem. Biol.* **19**, 198–205
15. Shoup, D., Roth, A., Puchalla, J., and Rye, H. S. (2022) The impact of hidden structure on aggregate disassembly by molecular chaperones. *Front. Mol. Biosci.* **9**, 915307
16. Müller, S., Dennemärker, J., and Reinheckel, T. (2012) Specific functions of lysosomal proteases in endocytic and autophagic pathways. *Biochim. Biophys. Acta* **1824**, 34–43
17. Lee, J., and Ye, Y. (2018) The roles of endo-lysosomes in unconventional protein secretion. *Cells* **7**, 198
18. Carlisle, C., Prill, K., and Pilgrim, D. (2017) Chaperones and the proteasome system: regulating the construction and demolition of striated muscle. *Int. J. Mol. Sci.* **19**, 32
19. Morán Luengo, T., Kityk, R., Mayer, M. P., and Rüdiger, S. G. D. (2018) Hsp90 breaks the deadlock of the Hsp70 chaperone system. *Mol. Cell* **70**, 545–552.e9
20. Gao, X., Carroni, M., Nussbaum-Krammer, C., Mogk, A., Nillegoda, N. B., Szlachcic, A., *et al.* (2015) Human Hsp70 disaggregase reverses Parkinson's-linked α-synuclein amyloid fibrils. *Mol. Cell* **59**, 781–793
21. Rohland, L., Kityk, R., Smalinskaitė, L., and Mayer, M. P. (2022) Conformational dynamics of the Hsp70 chaperone throughout key steps of its ATPase cycle. *Proc. Natl. Acad. Sci. U. S. A.* **119**, e2123238119
22. Kityk, R., Kopp, J., Sinning, I., and Mayer, M. P. (2012) Structure and dynamics of the ATP-bound open conformation of Hsp70 chaperones. *Mol. Cell* **48**, 863–874
23. Morshauser, R. C., Hu, W., Wang, H., Pang, Y., Flynn, G. C., and Zuiderweg, E. R. (1999) High-resolution solution structure of the 18 kDa substrate-binding domain of the mammalian chaperone protein Hsc70. *J. Mol. Biol.* **289**, 1387–1403
24. Pierpaoli, E. V., Sandmeier, E., Baici, A., Schönfeld, H. J., Gisler, S., and Christen, P. (1997) The power stroke of the DnaK/DnaJ/GrpE molecular chaperone system. *J. Mol. Biol.* **269**, 757–768
25. Moessmer, P., Suren, T., Majdic, U., Dahiya, V., Rutz, D., Buchner, J., and Rief, M. (2022) Active unfolding of the glucocorticoid receptor by the Hsp70/Hsp40 chaperone system in single-molecule mechanical experiments. *Proc. Natl. Acad. Sci. U. S. A.* **119**, e2119076119
26. De Los Rios, P., Ben-Zvi, A., Slutsky, O., Azem, A., and Goloubinoff, P. (2006) Hsp70 chaperones accelerate protein translocation and the unfolding of stable protein aggregates by entropic pulling. *Proc. Natl. Acad. Sci. U. S. A.* **103**, 6166–6171
27. Voisine, C., Craig, E. A., Zufall, N., von Ahsen, O., Pfanner, N., and Voos, W. (1999) The protein import motor of mitochondria: unfolding and trapping of preproteins are distinct and separable functions of matrix Hsp70. *Cell* **97**, 565–574
28. Shoup, D., and Priola, S. A. (2024) Grp78 destabilization of infectious prions is strain specific and modified by multiple factors including accessory chaperones and pH. *J. Biol. Chem.* **300**, 107346
29. Nillegoda, N. B., Kirstein, J., Szlachcic, A., Berynskyy, M., Stank, A., Stengel, F., *et al.* (2015) Crucial HSP70 co-chaperone complex unlocks metazoan protein disaggregation. *Nature* **524**, 247–251
30. Park, K.-W., Eun Kim, G., Morales, R., Moda, F., Moreno-Gonzalez, I., Concha-Marambio, L., *et al.* (2017) The endoplasmic reticulum chaperone GRP78/BiP modulates prion propagation in vitro and in vivo. *Scientific Rep.* **7**, 44723
31. Tuite, M. F., and Koloteva-Levin, N. (2004) Propagating prions in fungi and mammals. *Mol. Cell* **14**, 541–552
32. Meisl, G., Kurt, T., Condado-Morales, I., Bett, C., Sorce, S., Nuvolone, M., *et al.* (2021) Scaling analysis reveals the mechanism and rates of prion replication in vivo. *Nat. Struct. Mol. Biol.* **28**, 365–372
33. Saha, I., Yuste-Checa, P., Da Silva Padilha, M., Guo, Q., Körner, R., Holthusen, H., *et al.* (2023) The AAA+ chaperone VCP disaggregates Tau fibrils and generates aggregate seeds in a cellular system. *Nat. Commun.* **14**, 560

34. Tittelmeier, J., Sandhof, C. A., Ries, H. M., Druffel-Augustin, S., Mogk, A., Bukau, B., and Nussbaum-Krammer, C. (2020) The HSP110/HSP70 disaggregation system generates spreading-competent toxic α-synuclein species. *EMBO J* **39**, e103954
35. Sadlish, H., Rampelt, H., Shorter, J., Wegrzyn, R. D., Andréasson, C., Lindquist, S., and Bukau, B. (2008) Hsp110 chaperones regulate prion formation and propagation in S. cerevisiae by two discrete activities. *PLoS One* **3**, e1763
36. Shoup, D., and Priola, S. A. (2021) The size and stability of infectious prion aggregates fluctuate dynamically during cellular uptake and disaggregation. *Biochemistry* **60**, 398–411
37. Shoup, D., and Priola, S. A. (2023) Full-length prion protein incorporated into prion aggregates is a marker for prion strain-specific destabilization of aggregate structure following cellular uptake. *J. Biochem.* **174**, mvad032
38. Zhu, G., Harischandra, D. S., Ghaisas, S., Zhang, P., Prall, W., Huang, L., *et al.* (2020) TRIM11 prevents and reverses protein aggregation and rescues a mouse model of Parkinson's disease. *Cell Rep.* **33**, 108418
39. Huang, L., Agrawal, T., Zhu, G., Yu, S., Tao, L., Lin, J., *et al.* (2021) DAXX represents a new type of protein-folding enabler. *Nature* **597**, 132–137
40. Boellmann, F., Guettouche, T., Guo, Y., Fenna, M., Mnayer, L., and Voellmy, R. (2004) DAXX interacts with heat shock factor 1 during stress activation and enhances its transcriptional activity. *Proc. Natl. Acad. Sci. U. S. A.* **101**, 4100–4105
41. Chen, L., Brewer, M. D., Guo, L., Wang, R., Jiang, P., and Yang, X. (2017) Enhanced degradation of misfolded proteins promotes tumorigenesis. *Cell Rep.* **18**, 3143–3154
42. Chen, C., Sun, X., Xie, W., Chen, S., Hu, Y., Xing, D., *et al.* (2020) Opposing biological functions of the cytoplasm and nucleus DAXX modified by SUMO-2/3 in gastric cancer. *Cell Death Dis.* **11**, 514
43. Yoneyama, M., Iwamoto, N., Nagashima, R., Sugiyama, C., Kawada, K., Kuramoto, N., *et al.* (2008) Altered expression of heat shock protein 110 family members in mouse hippocampal neurons following trimethyltin treatment in vivo and in vitro. *Neuropharmacology* **55**, 693–703
44. Yasuda, K., Nakai, A., Hatayama, T., and Nagata, K. (1995) Cloning and expression of murine high molecular mass heat shock proteins, HSP105. *J. Biol. Chem.* **270**, 29718–29723
45. Kaneko, Y., Kimura, T., Kishishita, M., Noda, Y., and Fujita, J. (1997) Cloning of apg-2 encoding a novel member of heat shock protein 110 family. *Gene* **189**, 19–24
46. Berthenet, K., Boudesco, C., Collura, A., Svrcek, M., Richaud, S., Hammann, A., *et al.* (2016) Extracellular HSP110 skews macrophage polarization in colorectal cancer. *Oncoimmunology* **5**, e1170264
47. Colgan, S. P., Pitman, R. S., Nagaishi, T., Mizoguchi, A., Mizoguchi, E., Mayer, L. F., *et al.* (2003) Intestinal heat shock protein 110 regulates expression of CD1d on intestinal epithelial cells. *J. Clin. Invest.* **112**, 745–754
48. Tytell, M., Greenberg, S. G., and Lasek, R. J. (1986) Heat shock-like protein is transferred from glia to axon. *Brain Res.* **363**, 161–164
49. Hightower, L. E., and Guidon, P. T., Jr. (1989) Selective release from cultured mammalian cells of heat-shock (stress) proteins that resemble glia-axon transfer proteins. *J. Cell Physiol.* **138**, 257–266
50. Thackray, A. M., Lam, B., McNulty, E. E., Nalls, A. V., Mathiason, C. K., Magadi, S. S., *et al.* (2022) Clearance of variant Creutzfeldt-Jakob disease prions in vivo by the Hsp70 disaggregase system. *Brain* **145**, 3236–3249
51. Hrizo, S. L., Gusarova, V., Habiel, D. M., Goeckeler, J. L., Fisher, E. A., and Brodsky, J. L. (2007) The Hsp110 molecular chaperone stabilizes apolipoprotein B from endoplasmic reticulum-associated degradation (ERAD). *J. Biol. Chem.* **282**, 32665–32675
52. Polverino de Laureto, P., Taddei, N., Frare, E., Capanni, C., Costantini, S., Zurdo, J., *et al.* (2003) Protein aggregation and amyloid fibril formation by an SH3 domain probed by limited proteolysis. *J. Mol. Biol.* **334**, 129–141
53. Hubbard, S. J. (1998) The structural aspects of limited proteolysis of native proteins. *Biochim. Biophys. Acta* **1382**, 191–206
54. Spolaore, B., Bermejo, R., Zambonin, M., and Fontana, A. (2001) Protein interactions leading to conformational changes monitored by limited proteolysis: apo form and fragments of horse cytochrome c. *Biochemistry* **40**, 9460–9468
55. Bessen, R. A., and Marsh, R. F. (1992) Biochemical and physical properties of the prion protein from two strains of the transmissible mink encephalopathy agent. *J. Virol.* **66**, 2096–2101
56. Parchi, P., Zou, W., Wang, W., Brown, P., Capellari, S., Ghetti, B., *et al.* (2000) Genetic influence on the structural variations of the abnormal prion protein. *Proc. Natl. Acad. Sci. U. S. A.* **97**, 10168–10172
57. Huang, J., Cohen, M., Safar, J., and Auchus, A. P. (2021) Variably protease-sensitive prionopathy in a middle-aged man with rapidly progressive dementia. *Cogn. Behav. Neurol.* **34**, 220–225
58. Kim, C., Haldiman, T., Cohen, Y., Chen, W., Blevins, J., Sy, M. S., *et al.* (2011) Protease-sensitive conformers in broad spectrum of distinct PrPSc structures in sporadic Creutzfeldt-Jakob disease are indicator of progression rate. *PLoS Pathog.* **7**, e1002242
59. Hara, H., and Sakaguchi, S. (2020) N-terminal regions of prion protein: functions and roles in prion diseases. *Int. J. Mol. Sci.* **21**, 6233
60. Priola, S. A. (2018) Cell biology of prion infection. In *Handbook of Clinical Neurology*, Elsevier: 45–68
61. Glover, J. R., and Lindquist, S. (1998) Hsp104, Hsp70, and Hsp40: a novel chaperone system that rescues previously aggregated proteins. *Cell* **94**, 73–82
62. Greene, L. E., Saba, F., Silberman, R. E., and Zhao, X. (2020) Mechanisms for curing yeast prions. *Int. J. Mol. Sci.* **21**, 6536
63. Barbitoff, Y. A., Matveenko, A. G., and Zhouravleva, G. A. (2022) Differential interactions of molecular chaperones and yeast prions. *J. Fungi (Basel)* **8**, 122
64. Council, N.R. (2010) *Guide for the Care and Use of Laboratory Animals*. The National Acadamies Press, Washington, DC
65. Choi, Y. P., and Priola, S. A. (2013) A specific population of abnormal prion protein aggregates is preferentially taken up by cells and disaggregated in a strain-dependent manner. *J. Virol.* **87**, 11552–11561
66. Vascellari, S., Orrù, C. D., Hughson, A. G., King, D., Barron, R., Wilham, J. M., *et al.* (2012) Prion seeding activities of mouse scrapie strains with divergent PrPSc protease sensitivities and amyloid plaque content using RT-QuIC and eQuIC. *PLoS One* **7**, e48969
67. Wilham, J. M., Orrú, C. D., Bessen, R. A., Atarashi, R., Sano, K., Race, B., *et al.* (2010) Rapid end-point quantitation of prion seeding activity with sensitivity comparable to bioassays. *PLoS Pathog.* **6**, e1001217